Numerical model to characterize the thermal comfort in new eco-districts: methodology and validation through the canyon street case

KHALED ATHAMENA [a,b], JEAN FRANCOIS SINI [b], JULIEN GUILHOT [a], JEROME VINET [a]
MAEVA SABRE [a], JEAN-MICHEL ROSANT [b]

[a] Centre Scientifique et Technique de Bâtiment, 11 rue Henri Picherit - BP 82341 - 44323 NANTES Cedex 3 FRANCE
[b] Laboratoire de Mécanique des Fluides, UMR CNRS 6598, Ecole Centrale de Nantes, 1 rue de la Noë, BP 92101, F-44321 NANTES cedex 03, FRANCE
Khaled.Athamena@cstb.fr , Jean-François.Sini@ec-nantes.fr , Julien.Guilhot@cstb.fr , Jerome.Vinet@cstb.fr , Maeva.Sabre@cstb.fr , Jean-Michel.Rosant@ec-nantes.fr

Abstract: - In built-up areas, the urban structures affect the radiative and thermal environment. The numerical simulation models provide informations about urban thermal performance for many ranges of urban configurations. This paper presents a validation of a numerical approach based on the coupling of a CFD model (Code_Saturne software developed by E.D.F [1]) and thermo-radiative model (SOLENE software developed by CERMA laboratory [2]). The results of the coupled simulations are compared with in situ data obtained during EM2PAU [3] campaign. The experimental configuration was formed of two lines of steel containers buildings composing one street canyon. Thermocouples are fixed on the container surface temperature of the two canyon walls, roofs and ground. Shortwave radiation and net all-wave radiation are measured by three radiometers. Measurements of air temperature inside the containers, wind speed and direction are carried out and then used as boundary conditions in the coupling simulations. The simulated wind velocity and surface temperature are compared with the measurements for one day with clear sky conditions. The numerical coupling model developed will be later use for other studies aiming to characterize the comfort parameters for more realistic geometry of eco-districts.

Key-Words: - Coupling model, Thermo-radiative model, CFD model, Street canyon, Building heat transfers

1 Introduction

Control and improvement of architectural and urban ambient environment in relation to user comfort or air quality require a good knowledge of urban microclimate and its impact on the urban spaces. The urban microclimate results from a complex interaction between physical phenomena (wind, solar and infrared radiation...) and the nature of the object "city" which includes buildings, natural features (vegetation, water, soil ...), canopy morphology and human activity that develops within it.
Since 20 years, the thermal environment of urban areas has been characterized by urban heat island phenomenon (UHI) effects **[1]**. The urban heat island is the most evident result of climatological phenomena caused by urbanization, whose result is an increase of urban air temperature **[2]**.
The objects of urban environment, including buildings, urban geometry, materials and vegetation, play an important role in the urban microclimate and the conditions of thermal comfort **[3]**. Many urban forms have been studied by researchers: urban street canyon **[1, 4]** parallel and staggered rows **[5]**, slab and pavilion-court **[6].**
We are interested on a new generation of urban configuration known as "eco-districts" or "sustainable districts". In these new spaces, planners have promoted the emergence of a new approach to design, build, operate and manage the urban space. Among these different configurations of eco-district which ones can be retained or adapted to produce a coherent urban form in order to answer the environmental challenges?

---
[1] Electricité De France
[2] Centre de Recherche Méthodologique d'Architecture
[3] Influence des Effets Micro-Météorologiques sur la Propagation Acoustique en milieu Urbain. Running experiment (2009-2011) in Nantes

ISBN: 978-960-474-268-4

Nomenclature

ε_i	Emissivity of element i
λ	Thermal conductivity [W/m/K]
ρ	Density [kg/m^3]
κ	Von Karman constant
σ	The Stefan–Boltzmann constant
φ_{sol}	Solaire flux density [W/m²]
φ_{LW}	Long wave Flux density [W/m²]
a	Albedo [–]
Cp	Specific heat [J/kg/ K]
h	Sensible heat transfer coefficient [W/m²/ K]
d	Thickness [m]
W	Street width [m]
H	Building height [m]
V	Average axial airflow velocity within the canyon [m/s]
T_i	Temperature of element i
Tair	Air temperature

Thermal comfort parameters (surface temperature, wind and air temperature, radiation) and comfort indicators (PET or PMV*) for several eco-districts configurations must be defined and characterized.

Numerical simulation models provide informations about urban thermal performance for a range of urban configurations [7]. These models are divided into two categories:

- Computational fluid dynamics (CFD) models which compute air temperatures, wind and turbulence around the buildings and require the surface temperature as input parameter,
- Thermo-radiative models which calculate the thermo-radiative balance and surface temperature of buildings, ground and require the wind speed close to the surface for the convective heat flux determination.

Usually, in urban CFD simulations, homogeneous values of surface temperature are used to compute wind, air temperature and turbulence in the canopy layer. On the other hand, a unique reference wind speed and uniform value are generally used to compute wall and ground temperatures in thermo-radiative models. However, in outdoor spaces, the distribution of these parameters is far from uniform and shows large deviations from one building façade to another. A two-way coupling of dynamic and thermo-radiative models would avoid many crude approximations that result in separated model applications, and thus certainly improve the quality of simulation results.

In this article a coupling between a thermo-radiative software (SOLENE developed by CERMA) and a CFD software (Code_Saturne developed by E.D.F) is presented.

Results of the coupled simulations are compared with experimental data selected from the surface temperature and air velocity measurements of the EM2PAU in situ campaign. In these simulations, it is assumed that anthropogenic heat flux and latent heat flux are negligible.

2. Numerical modeling

2.1. The thermo-radiative model SOLENE

SOLENE is dedicated to the simulation of solar and infrared radiation in urban environment [8] at different scales ranging from buildings and streets to urban district. SOLENE includes many modules for determining the lighting parameters such as sky factors and daylight factors on urban scene etc. The radiative transfer modeling in SOLENE is divided in

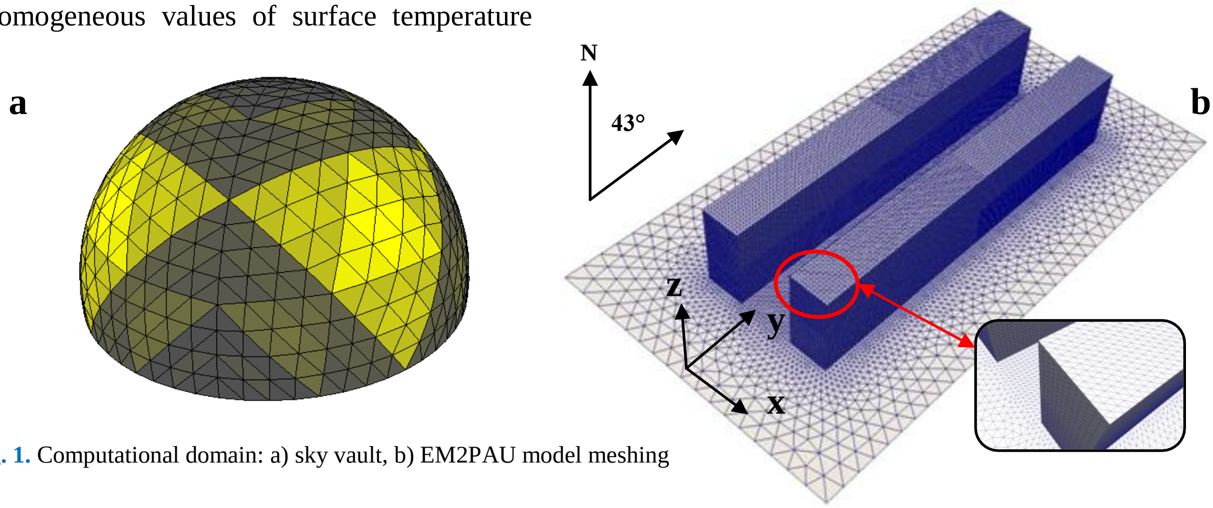

Fig. 1. Computational domain: a) sky vault, b) EM2PAU model meshing

solar and long-wave radiation. For each element of the urban scene (buildings, ground, etc.), global solar contribution is computed as a sum of the direct, diffuse and reflected irradiances. These contributions are used to initialize a progressive refinement algorithm which treats the inter-reflections between surfaces of the urban scene in order to obtain the net solar radiation flux [8].

Long-wave radiative exchanges, R_{LW}, between the facets of the urban scene are computed by using surfaces view factor distribution, $F_{i,j}$:

$$R_{LW} = \sum_{j=1}^{n} \varepsilon_i F_{i,j} \sigma (T_i^4 - T_j^4) \qquad (2)$$

The long-wave radiation exchanged between the facets and the sky is determined by using the sky view factor $F_{i,sky}$:

$$R_{sky} = F_{i,sky} \sigma \varepsilon_i (T_i^4 - L_\downarrow) \qquad (3)$$

When $L_\downarrow$ is the sky radiation that can be expressed as a function of air temperature [9] :

$$L_\downarrow = 213 + 5.5\, T_{air} \qquad (4)$$

In addition, the wall model in SOLENE is modeled by only two superimposed layers, an external on in contact with atmosphere, and an internal on. The wall model is based on the electrical analogy of resistances and thermal capacities. We also note that, exchanges of energy are mono-dimensional and bidirectional (towards inside or outside) [10].

SOLENE inputs are the date (day and time), the meteorological data (air temperature, wind speed, nebulosity or cloud coverage), temperatures inside the buildings and ground deep layer. The software allows outputting of all surface temperatures and energy fluxes, as well as the integral fluxes through a horizontal surface between the scene and the sky.

2.2. The airflow model Code_Saturne

Code_Saturne is a system designed to solve the Navier-Stokes equations. It is based on a co-

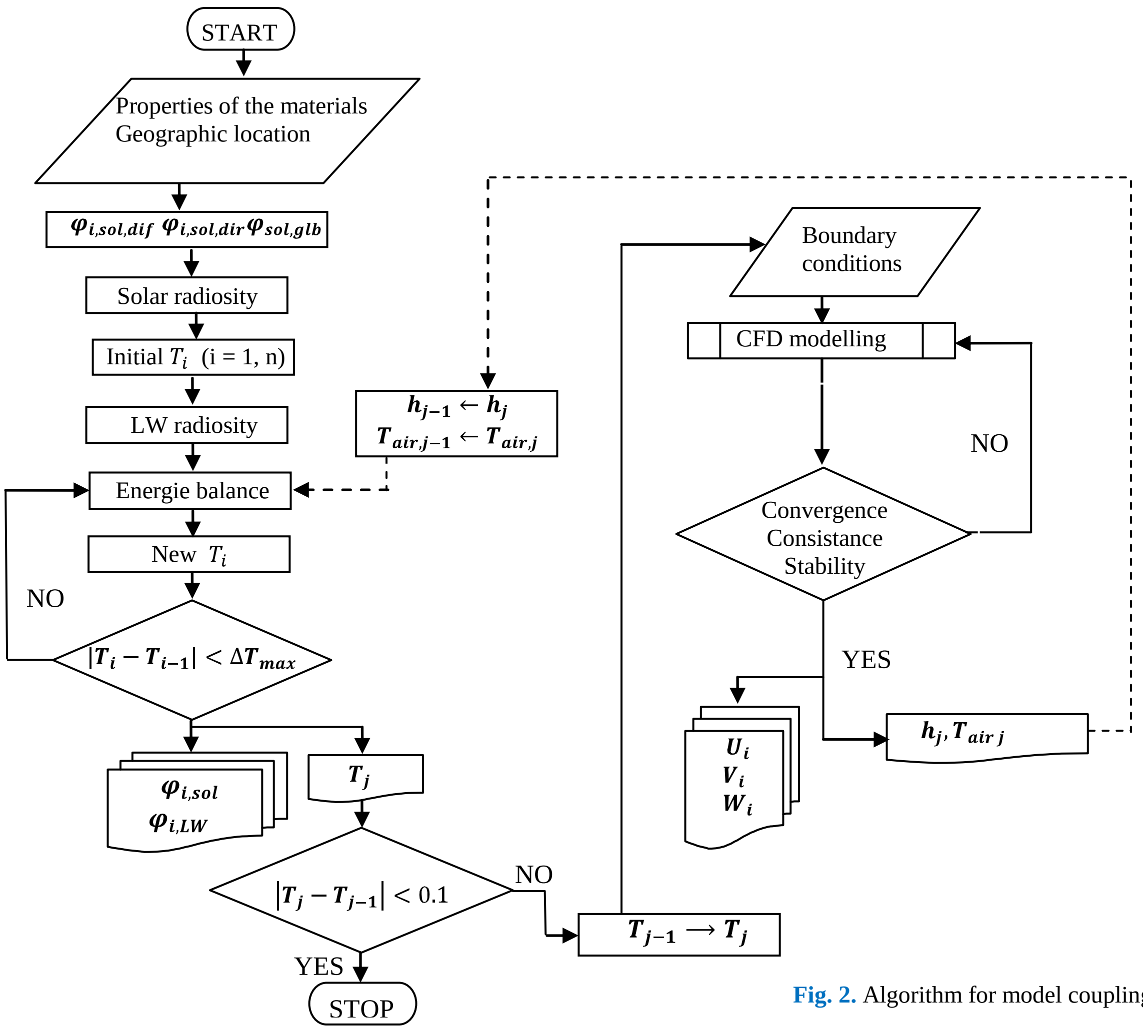

Fig. 2. Algorithm for model coupling

located finite volume approach that accepts meshes with any type (tetrahedral, hexahedral, prismatic, pyramidal, polyhedral...) and any type of grid structure (unstructured, block structured, hybrid, conforming or with hanging node). Its main module is designed for the simulation of flows which may be steady or not, laminar or turbulent, incompressible or potentially dilatable, isothermal or not. Scalars and turbulent fluctuations of scalars can be taken into account.
Code_Saturne was designed for industrial simulation. Many internal subroutines were adapted to carry more representative simulations of urban reality (Logarithmical wind profile, physical characteristics of the air flow, added source / sink terms in momentum and turbulent energy equations to take into account the vegetation in the simulation). Equations of $k-\varepsilon$ standard model of turbulence, Boussinesq hypothesis and Sutherland law for thermal model are used.

2.3 Methodology for coupling the models

The principle of the coupling consists in an information exchange in both ways between the two numerical models at each time-step of computation. Surface temperatures (*Tj*) are calculated by the thermo radiative balance of SOLENE and introduced on Code_Saturne as boundary conditions. The thermo-dynamic simulation, carried out by Code_Saturne, computes air temperature (Tair) and convective exchange coefficients (h), which are reintroduced in SOLENE as input data. The coupling between SOLENE and Code_Saturne goes on until fixed convergence criteria are reached. In our study, convergence criteria correspond to a maximal difference of 1 °C on a given cell and a maximum of 0.1 °C on the temperature averaged over the wall domain calculated at two successive iterations.
Radiation and thermal models, implemented in SOLENE model, use surface meshes. The airflow model, implemented in Code_Saturne, uses volume grid. In order to facilitate data transfer between the radiation model and the airflow model, the same surface grid was used. In this research, many adaptations are carried out by thermo-dynamic simulation in Code_Saturne. The convective exchange coefficient (h) is calculated by standard walls laws adapted for industrial applications but not for urban applications because boundary layers have not the same scale. In our research, an empirical law **[11]** applicable to the urban environment is used to adapt the value of h at each cell. This law allows restoring h for air velocity (V)

$$h = 11.8 + 4.2\,V \qquad (5)$$

The algorithm of numerical coupling model is presented in **[Fig. 2]**

3. Validation measurements

3.1. The measurements

The EM2PAU experiment was conducted at the experimental site of the LCPC (Laboratoire Central des Ponts et Chaussées) about 13 km west from Nantes in France (47°12'N, 1°33'W). Two rows of buildings in a street canyon shape were installed on experimental site. Each line was composed of four empty steel containers and have in length L = 24 m, H = 5.2 m in height and B = 2.45 m in width. The street width was W = 3.64 m. The aspect ratio W/H was approximately 0.70, a typical value in, e.g., historical centre of old European cities and medina's of north Africa and Middle East cities. This morphological parameter corresponds of

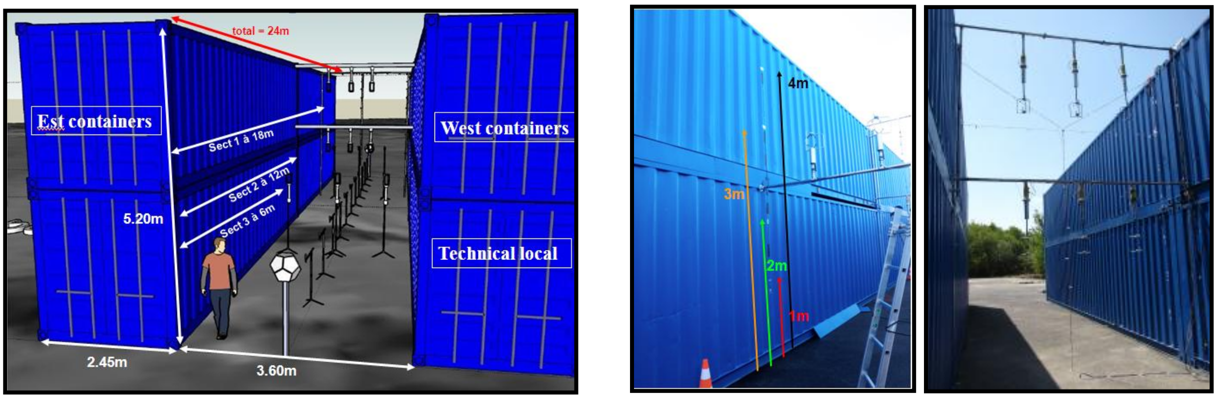

Fig. 3. EM2PAU experimental site: a) model dimension, b) 3D sonic anemometer in the street central section, c) thermocouples glued at the steel surface

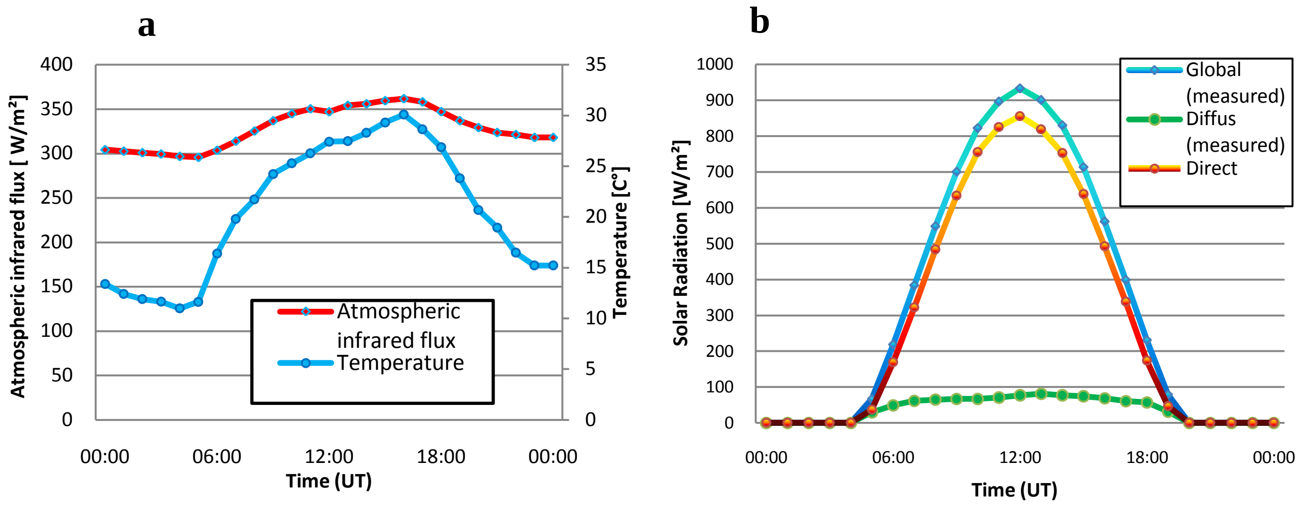

Fig. 4. Reference meteorological conditions: a) ambient air temperature, atmospheric infrared flux (measured), b) solar radiation.

narrow street canyon geometry. The street axis formed an angle of 43° with the north [Fig. 1].

The experiment was installed on a stabilized ground of 0.05 m of asphalt layer over the compacted natural soil. The measurement period is schedule for 18 months between March 2010 and October 2011.

Thermo-radiative instrumentations and anemometers included the following sensors in the central part of the street:

- Two lines of 32 thermocouples, glued at the steel surface, to measure vertical temperature profile on the two canyon walls,
- A set of 8 thermocouples to monitor air temperature inside the containers,
- 3 radiometers viewing the sky were set on the roof of west containers, 2 pyranometers measured the shortwave radiation and 1 pyrgeometer measured the infrared radiation.
- The air velocity inside canyon is measured by 6. 3D sonic anemometers clamped in the mid-street vertical section.
- Wind speed and direction are measured at the top of a 10 m mast.

	d(m)	a(-)	ε (-)	λ (W/m²/K)	Cp (j/kg/K)	ρ (Kg/m³)
Canyon walls & roofs – upper and lower containers						
Steel	0.025	0.20	0.95	45.3	500	7830
Technical local						
Steel*	0.025	0.20	0.95	45.3	500	7830
Air layer	0.15	-	-	0.04	1.25	1000
Polystyrene	0.45	-	-	0.032	35	1450
Ground						
Asphalt	0.05	0.17	0.95	2.4	1600	950
Soil	0.70	-	-	1.3	1600	900

Table. 1. Physical properties of street canyon materials (see nomenclature).
* - neglected in calculation.

These data were averaged and stored every 15 min with the meteorological data.

2. The Data

The data selected for the model validation correspond to the 7th of July 2010, a hot day with clear sky conditions. Simulations are computed for a period of 24 hours with 15 min time step. Meteorological data of July 7th are displayed in [Fig. 4]. Measured global and diffuse solar radiation and infrared thermal radiation from the atmosphere L↓ measured on a horizontal plane were used as an input data. This one was computed with subtracted the global radiation to diffuse radiation. Temperatures measured inside the containers and within the soil at the depth of 0.70 m were also used in the simulation as a boundary condition for the conductive heat transfers through the wall and the soil. During the diurnal cycle, they varied from 14 °C to 43 °C in the upper containers and from 9 °C to 52 °C in the lower containers. The soil temperature varied little from 21 °C to 23 °C. The heat transfer coefficient inside the containers was set at 10 W/m²/K, a usual value for a closed room.

4. Model Validation:

4.1. Model set-up

The computational domain is composed of long building lines and the ground surface. For thermo-radiative simulation, the ground is composed of two layers (asphalt and soil). All canyon walls and roofs were modeled with a single 0.025 m steel layer except technical local

ISBN: 978-960-474-268-4

installed in the lowest part of west containers for computers of acquisition **[Fig. 3, a].** This one was modeled with two layers: the 0.45 m extruded polystyrene layer and 0.15 m air layer. The 0.025 mm steel walls are not modeled since, due to its very high heat conductivity and low capacity, its temperature appears always very close to the air layer.
The values of physical properties **[Table. 1]** were selected from the ASHRAE Handbook **[12, 13]** to best reproduce the used materials. A grid of 42 412 triangular meshes, 0.02 m² in size was used for surface and 1024 triangular meshes for the hemispheric sky vault **[Fig. 1, a&b]**. Solar irradiances were computed with the clear sky model of Perez et al. **[18]**. Simulations were carried out with a 15 min time step for the period of 24 h.

For dynamic simulation, inlet wind profile is **[14]**

$$U(z) = \frac{U^*}{\kappa} \ln\left(\frac{z}{z_0}\right) \qquad (6)$$

In this research, empirical values of Roughness length [z_o] following the nature of experimental site were imposed. With velocity of wind measured at the top of a 10 m mast, the friction velocity [U^*] was calculated. These data enable to reconstitute the inlet wind profile at each time step of simulations.

4.2 Comparison to measurements

4.2.1 Surface temperature

[Figs. 5 and 6] present a comparison of the simulated surface temperature values with the measurements of July 7th. Vertical lines indicate the time when walls start being sunlit (dash lines) and shadowed (solid lines) at the sensor locations. Temperature measurements are displayed at the roof (z/H = 1), walls elements (z/H = 0.77, 0.57 and 0.38, respectively), and at ground level (z/H = 0) **[Fig .5]**.

Results show a good similarity between simulations and measurements for containers walls. It can be attributed to the low thermal inertia of walls modeled with small 25 mm thick steel.
Considering the simulation conditions (clear sky), roofs are the only parts of model which see the solar radiation during the day from 6:00 to 18.00 (UT) and which present the higher temperatures. The results of roofs simulation match quite well the measurements, with a tendency to a slight underestimation during high sunlit from 10:00 to 16:00 (UT) **[Fig; 6 A and E]**.
For walls, the western part **[Fig. 6, B, C, D]** starts being sunlit at sunrise (04:30 UT). The thermocouples of the upper level are the first ones to receive morning sun radiation. They remained sunny from 04:30 to 10:00 (UT). The thermocouples of the lower level see the sun from 04:30 to 06:30 (UT) then they skip in the shade arise from containers in front of. Then they see again sun radiations until 11.30 (UT). The lower measurement levels are back in the shadow while the upper levels remain sunlit.
The eastern parts **[Fig. 6, F, G, H]** are sunlit during a part of the afternoon, from 13:30 to 17.30 (UT). Due to the actual orientation (43 ° north), the upper part of the wall is sunlit for a longer period than the lowest one.
Wall temperatures clearly show two maximum during the sunlit period and also a secondary peak when the opposite wall is sunlit due to solar radiation reflection. Yet, the opposite wall behaviors are not symmetrical due to the differences in air temperature and infrared atmospheric flux between the morning and afternoon.
At the ground **[Fig. 5]**, a small deviation between simulation results and measurements was showed in the morning and in the afternoon. An overestimation of Asphalt albedo is the probable cause of this deviation.

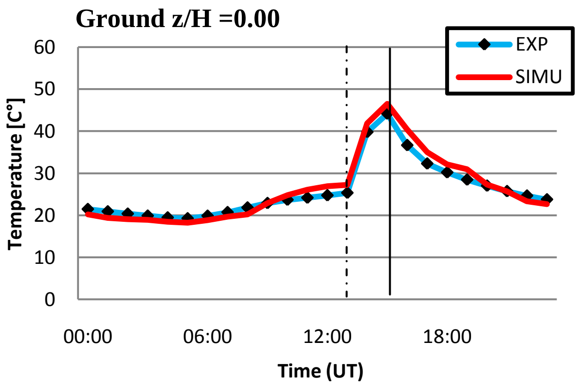

Fig 5. Ground surface temperature simulation versus measurement

4.2.2 Air velocity:

[Figs. 7] present the comparison of the simulated air velocity values with the

Fig 6. Roofs and walls surface temperature simulation versus measurement

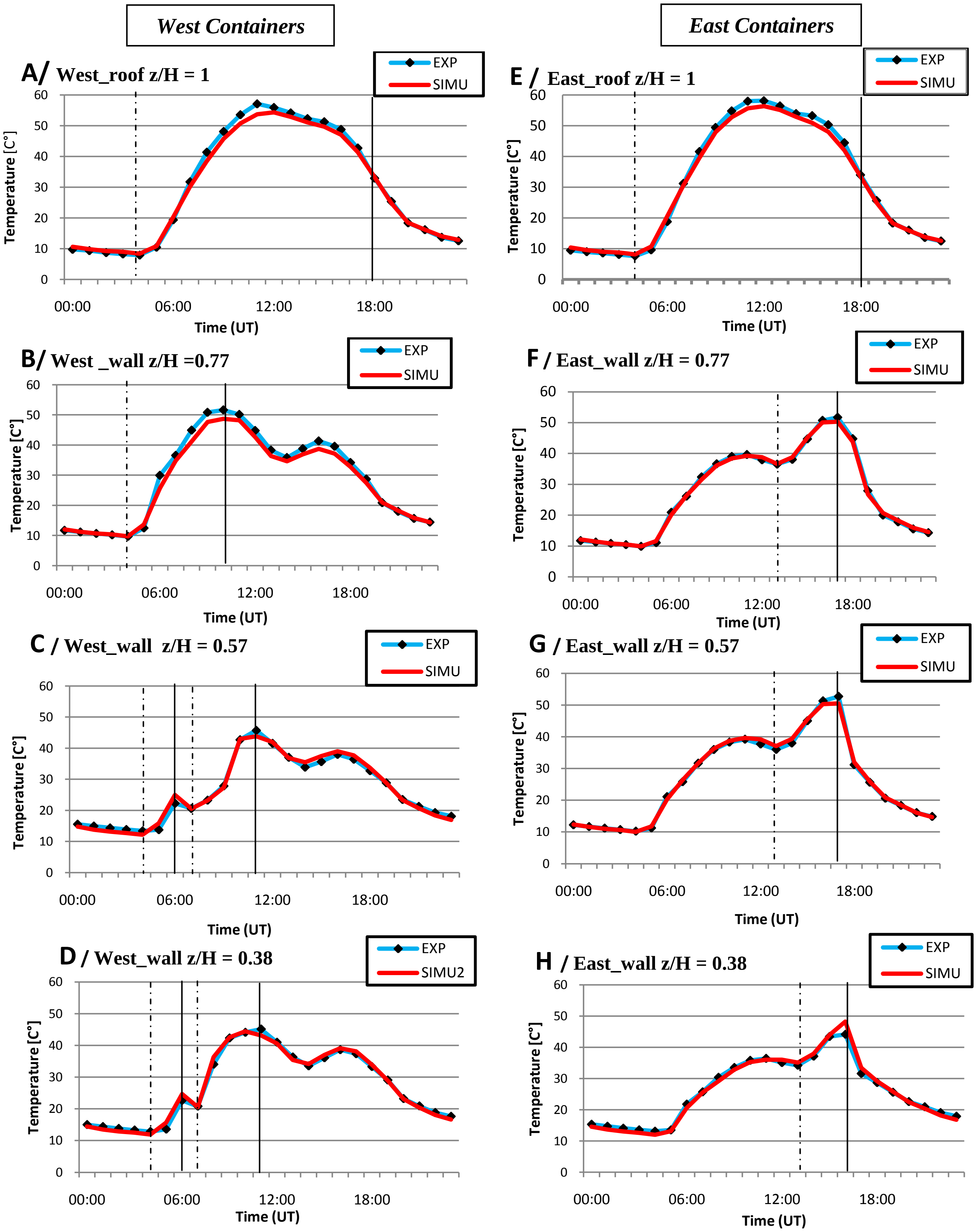

measurements inside the canyon. Results compared concern two 3D sonic anemometers placed at different heights: the first near east containers at z/H = 0.77 and the second in the middle of street canyon at z/H = 0.36.

Results show an underestimation of measurements compare to simulations, especially for V component (along the street axis).

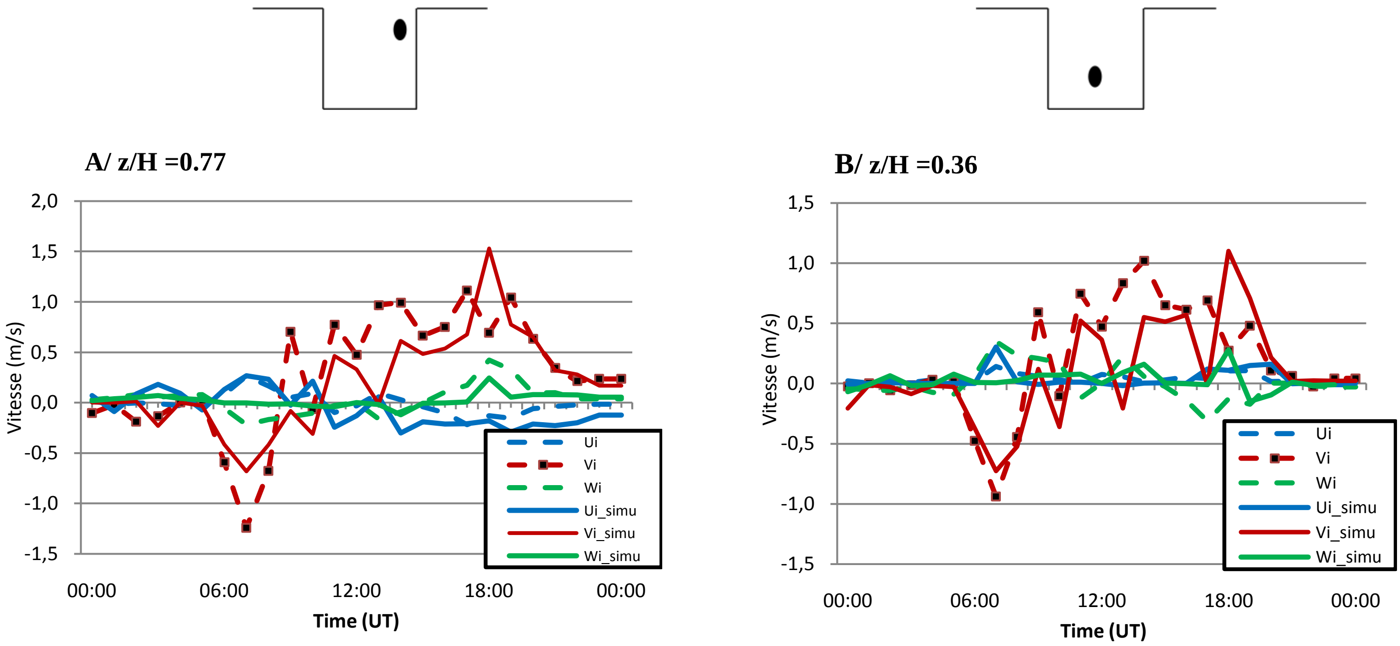

Fig. 7. Air velocity simulation versus measurement at two differnces level inside the street canyon

We think that this may be due to the inlet wind profile reconstituted at each time from values of wind velocity measured at the top of a 10 m mast and empirical values of roughness length [zo]. This might be responsible for an underestimation of velocity value in the lower part of the inlet wind profile. It is very difficult to make comparison of numerical result with local measurement in real site.

5. Conclusion:

A numerical model, based on the coupling of the airflow and thermal radiation was developed for the simulation of dynamic and heat transfer in urban area. In principle, the approach can be useful for complex geometry and for the analysis of comfort thermal environment since it can provide air temperature, wind velocity and radiation conditions in urban environment. Hence, the model appears reliable to predict solar and thermal radiation. However, for wind velocity, results present significant deviations probably due to the boundary conditions.

The detailed analysis of the results study shows that the selection of boundary conditions for dynamic simulation and the material parameters, thermal conductivity, heat capacity, albedo, emissivity for thermo radiative simulation, is a key of the simulation quality.

Acknowledgements

We would like to thank the regional council of Pays de la Loire for financing the EM2PAU research project and LCPC for sharing the experiment data base.

References:

[1] Oke, T. R. (1988). "*Street design and urban canopy layer climate.*" Energy and Buildings 11(1-3), pp. 103--113.

[2] Akbari, H. et S. Konopacki (2004). "*Energy effects of heat-island reduction strategies in Toronto, Canada*." Energy and Building 29(2), pp. 191--210.

[3] Santamouris, M., N. Papanikolaou, I. Livada, I. Koronakis, C. Georgakis, A. Argiriou et D. N. Assimakopoulos (2001). "*On the impact of urban climate on the energy consumption of buildings*." Solar Energy 70(3), pp. 201-216.

[4] Ali-Toudert F, Mayer H. (2007). "*Thermal comfort in an east–west oriented street canyon under hot summer conditions*". Building and Environment 41(2), pp. 94--108.

[5] Shashua-Bar, L., M. E. Hoffman et Y. Tzamir (2006). "*Integrated thermal effects of generic built forms and vegetation on theUCL microclimate*." Building and Environment 41(3), pp. 343--354.

[6] Ratti, C., D. Raydan et K. Steemers (2003). "*Building form and environmental performance: archetypes, analysis and an arid climate."* Energy and Buildings 35(1), pp. 49--59

[7] Masson, V., C. S. B. Grimmond, and T. R. Oke, (2002): "*Evaluation of the Town Energy Balance (TEB) scheme with direct measurements from dry districts in two cities*". J. Appl. Meteor., 41, 1011–1026.

[8] Miguet, F., Groleau, D., 2002. "*A daylight simulation tool for urban and architectural spaces. Application to transmitted direct and diffuse light through glazing*". Building and Environment 37, 833–843.

[9] Monteith, J.L., Unsworth, M.H., 1991. "*Principles of Environmental Physics"*. Edward Arnold, New York.

[10] Vinet, J., 2000. "*Contribution à la modélisation thermo-aéraulique du microclimat urbain. Caractérisation de l'impact de l'eau et de la végétation sur les conditions de confort en espaces extérieurs*". Phd. Thesis. Nantes, Université de Nantes.

[11] Rowley FB, Algren AB, Blackshaw JL. "*Surface conductances as affected by air velocity, temperature and character of surface*". ASHRAE Trans 1930; 38:33–46.

[12] ASHRAE handbook, fundamentals. Atlanta, Georgia: ASHRAE; 2001. pp. 36.1–36.4.

[13] Mazria. E. "*Le guide de l'énergie solaire passive*", Parenthéses1979. P 272-277.

[14] C.S.T.B. " *traité de physique de bâtiment, connaissance de base. Tome : 1"*, CSTB. P 718-719.